Thermal characterization, polymorphism, and stability evaluation of Se-NSAID derivatives with potent anticancer activity

Sandra Ramos-Inza[1,2] · Eneko Almagro[3] · María Font[1,2] · Ignacio Encío[2,4] · Daniel Plano[1,2] · Carmen Sanmartín[1,2] · Rafael Sirera[3] · Elena Lizarraga[1]

Abstract

Stability, thermal characterization, and identification of possible polymorphism are relevant in the development of novel therapeutic drugs. In this context, thirty new nonsteroidal anti-inflammatory drug (NSAID) derivatives containing selenium (Se) as selenoesters or diacyl diselenides with demonstrated anticancer activity were thermally characterized in order to establish thermal stability criteria and detect possible polymorphic forms. Compounds were analyzed by a combination of thermogravimetry, differential scanning calorimetry, and X-ray diffraction techniques, and five different calorimetric behaviors were identified. Two compounds based on naproxen (**I.3d** and **I.3e**) and an indomethacin-containing derivative (**II.2**) presented two crystalline forms. The stability under acid, alkaline and oxidative conditions of selected polymorphs was also assessed using high-performance liquid chromatography. In addition, the cytotoxic activity of Se-NSAID crystalline polymorphs was studied in several cancer cell lines in vitro. Remarkably, no significant differences were found among the polymorphic forms tested, thus proving that these compounds are thermally qualified for further drug development.

Graphical abstract
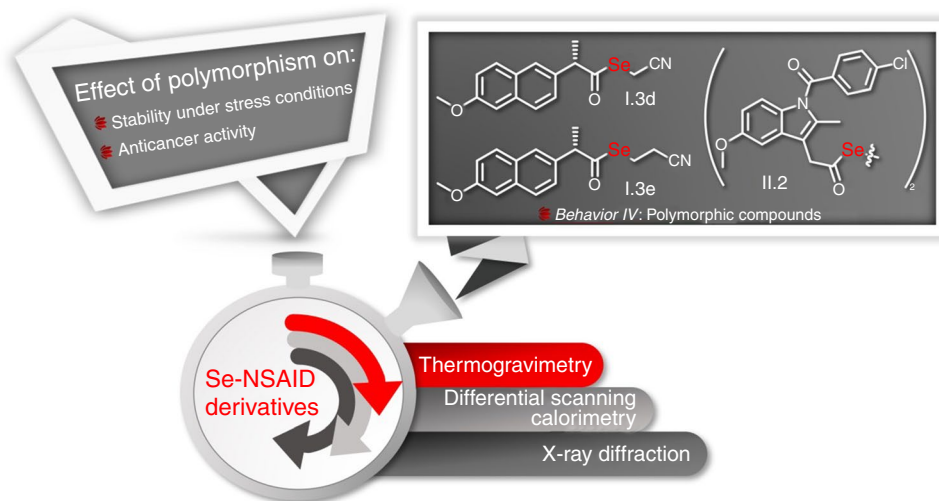
Keywords Selenium · NSAID · Polymorphism · TG/DSC analysis · X-ray diffraction · Cytotoxicity

Abbreviations

ASA	Aspirin
ATCC	American Type Culture Collection
DSC	Differential scanning calorimetry
FBS	Fetal bovine serum

Rafael Sirera, Elena Lizarraga: same contribution and supervision as senior authors.

Extended author information available on the last page of the article

FDA	Food and Drug Administration
HPLC	High-performance liquid chromatography
HRMS	High-resolution mass spectrometry
Ibup	Ibuprofen
ICH	International Conference on Harmonization
Ind	Indomethacin
Ket	Ketoprofen
MTT	3-(4,5-Dimethylthiazol-2-yl)-2,5-diphenyltetrazolium bromide
Nap	Naproxen
NMR	Nuclear magnetic resonance
NSAIDs	Nonsteroidal anti-inflammatory drugs
Salic	Salicylic acid
Se	Selenium
TG	Thermogravimetry
UV	Ultraviolet
XRD	Powder X-ray diffraction

Introduction

Polymorphism is defined as the ability of a certain substance to crystallize in two or more crystalline phases with different arrangements or conformations of the constituents in the crystal lattice [1]. Significant differences in chemical and physical characteristics may arise with the associated changes in the solid-state form, such as chemical stability [2], bioavailability, solubility [3], melting point, hygroscopicity, morphology, and density, thus affecting the behavior and properties of the compound [1]. Polymorphism is a frequently encountered problem faced by industry during the production of commercial pharmaceutical formulations that can alter physicochemical properties of resulting end-products [4], since different polymorphic forms can be produced by standard pharmaceutical processes such as crystallization, milling, and heating [5]. Moreover, polymorphism is of great consideration since it could also affect the pharmaceutical performance of a drug [6]; and in an extreme case, an undesired polymorph can even have toxic effects [7]. Hence, the Food and Drug Administration (FDA) [7] and other regulatory agencies such as the International Conference on Harmonization (ICH) [8] require close attention to crystal polymorphism to ensure the quality of pharmaceutical compounds [3]. Therefore, the determination of polymorphic forms in the early stages of drug development provides valuable information, given that the synthetic process can be designed to isolate the crystalline form with the best characteristics in terms of biological activity and bioavailability.

In this context, thermal characterization [9–12] and stability [13] studies are of great interest in the chemical development of a compound with therapeutic properties. Methods such as thermogravimetry (TG) and differential scanning calorimetry (DSC) have been widely used in the preclinical development of pharmacologically active derivatives [1]. The determination of amorphous and crystalline forms can be achieved by powder X-ray diffraction (XRD) [12, 14, 15], and its combination with thermal methods allows the identification of polymorphic forms in therapeutic compounds [16, 17].

Nonsteroidal anti-inflammatory drugs (NSAIDs) have been traditionally known for their analgesic, anti-inflammatory, and antipyretic effects [18], but several epidemiological, preclinical, and clinical studies have supported their chemopreventive and chemotherapeutic potential for cancer treatment in recent years [19–23]. In this context, several efforts have been made to modify NSAID scaffolds to minimize possible side effects such as gastrointestinal [24] and cardiovascular [25] risks associated with their prolonged use, and to develop more effective drugs with novel mechanisms of action [26]. Likewise, the existence of some polymorphic forms of NSAIDs and NSAID derivatives has been identified [27–29]. For instance, both flufenamic [30] and tolfenamic [31] acids presented nine polymorphs each, respectively, and aceclofenac was reported to have at least six polymorphs [32]. Aspirin also presented at least two stable polymorphic forms [33], while eight polymorphs have been identified for indomethacin [34]. Thermal characterization of different NSAIDs has also been reported [35–39], but to the best of our knowledge, no study regarding thermal analyses of organic modified-NSAID derivatives with a demonstrated antiproliferative activity has been reported to date in the literature.

Additionally, a plethora of evidence supports the role of Se in preventing cancer incidence and blocking tumor metastasis [40]. Accordingly, Se-containing compounds have been considered appealing agents in the field of drug discovery for cancer therapy over recent decades [41–43]. Hence, their potent anticancer activity has been demonstrated in xenograft models [44, 45] involving several mechanisms of action [42, 46, 47].

In this context, we have recently reported the development of new NSAID analogs based on the combination of NSAID scaffolds and different Se entities, thus obtaining potent and selective compounds for the treatment of breast [48] and colon cancers. Thermal characterization and studies on polymorphism have also been performed on Se-containing compounds [16, 17, 49–52]. Thus, as a continuation of our purpose for developing new antitumoral drugs, we encompass in this work the thermal behavior evaluation and preliminary stability studies of a series of Se-NSAID derivatives with appealing anticancer properties, with the aim of establishing thermal stability criteria and studying their possible polymorphism. This research was carried out using TG, DSC, and XRD techniques, whereas the stability under stress conditions such as acid, alkaline, and oxidative

media was also assessed using HPLC/UV-DAD. In addition, an analysis has been carried out using molecular modeling techniques, in order to obtain data that help to interpret the thermal behavior and stability results of the target compounds. Furthermore, the cytotoxic effect of identified crystalline polymorphic forms was evaluated in a panel of cancer cell lines.

Experimental

Materials

A total of thirty compounds synthesized in the Department of Pharmaceutical Technology and Chemistry of the University of Navarra have been included in this work. Compounds are derived from NSAIDs including Se with different structural modifications. The selected NSAIDs were considered based on a variety of chemical structures with reported chemotherapeutic activity, such as aspirin (ASA), salicylic acid (Salic), indomethacin (Ind), naproxen (Nap), ketoprofen (Ket), and ibuprofen (Ibup).

The selenocompounds are divided into two series according to the chemical form in which Se was incorporated into the NSAID scaffold. Thus, series I comprised a total of twenty-five selenoesters decorated either with carboxylic functionalities in the form of carboxylic acids (**a**), esters (**b**), and amides (**c**), or with nitrile groups in hydrocarbon chains of different elongation with one (**d**) or two (**e**) methylene groups (Fig. 1a). Series II encompassed five compounds that were obtained as diacyl diselenides involving two moieties of the corresponding NSAID forming a symmetric molecule, as shown in Fig. 1b. The structures of all the compounds were confirmed by high-resolution mass spectrometry (HRMS) and by ^{1}H, ^{13}C and ^{77}Se nuclear magnetic resonance (NMR). The purity of key compounds was determined by reverse phase high-performance liquid chromatography (HPLC). All compounds are > 95% pure by HPLC analysis or quantitative NMR.

Chemistry

The synthesis of the thirty Se-NSAID derivatives analyzed in this work was achieved following similar synthetic routes. Briefly, selenoesters of series I were obtained by the reaction of the NSAID acyl chloride with an aqueous solution of sodium hydrogen selenide (NaHSe) formed in situ, followed by the addition of the
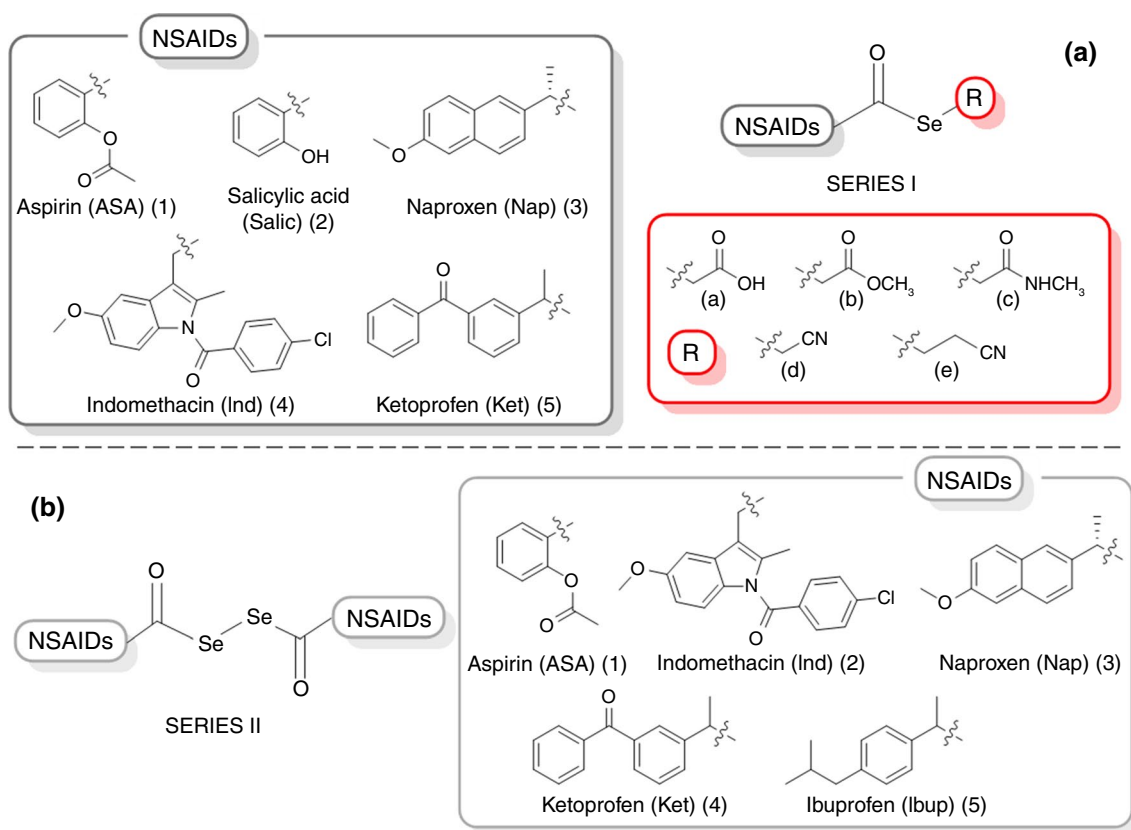
Fig. 1 General structure of the Se-NSAID derivatives based on **a** selenoesters (series I) or **b** diacyl diselenides (series II) included in this study

corresponding bromide with different terminations as previously described [48]. Diacyl diselenides of series II were obtained similarly to series I, but no additional reagent was added to the mixture of the NSAID acyl chloride and NaHSe prior to the workup of the reaction. In some cases, the NSAID acyl chloride was not commercially available and had to be synthesized by the reaction of the carboxylic acid reagent with oxalyl chloride in methylene chloride.

Products were purified by silica gel column chromatography or flash chromatography with a gradient of hexane and ethyl acetate as the elution solvent. ^{1}H, ^{13}C, and ^{77}Se NMR spectra were recorded on a Bruker Avance Neo 400 MHz operating at 400, 100, and 76 MHz, respectively, using TMS as the internal standard and CDCl$_3$ as solvent. HRMS was performed on a Micromass Q-TOF mass spectrometer. All the compounds were synthesized with a high grade of purity as they had been previously evaluated for their appealing anticancer potential in biological assays [48].

Thermal analysis

Thermogravimetric measurements were carried out using a SDT 650 TA Instrument equipment. The thermobalance and the oven temperatures were calibrated automatically. Approximately, 5 mg of each sample was placed in alumina crucibles of 90 μL and heated from 35 to 400 °C at a heating rate of 10 °C min^{-1} under N$_2$ atmosphere with a gas flow of 100 mL min^{-1}. The thermal values of the degradation process (T_{onset} and T_{max}), as well as their associated mass losses were calculated using a Trios TA Instrument software.

Calorimetric analyses were performed using a differential scanning calorimetry DSC 25 TA Instrument. Samples of approximately 5 mg were analyzed in aluminum capsules of 40 μL closed hermetically under N$_2$ atmosphere with a gas flow of 50 mL min^{-1}. In order to detect polymorphism, the calorimetric analyses started with the study of the thermal behavior of the Se-NSAID derivatives before their degradation process. Thus, samples of all the compounds were exposed to successive heating and cooling cycles. Compounds were heated at a heating rate of 10 °C min^{-1} from 25 °C to a temperature 20 °C below the T_{onset} of the degradation process to ensure that the Se-NSAID derivatives were not degraded. The resulting melted samples were then left to cool at room temperature to allow recrystallization of the compounds before continuing the thermal process. If polymorphism was detected, additional heating–cooling cycles were performed on the samples. Results were analyzed with a Trios TA Instrument software to obtain the values of T_{onset}, T_{max}, and the enthalpy of fusion ΔH_f of the selenocompounds.

Powder X-ray diffraction

Powder X-ray diffraction (XRD) patterns of the Se-NSAID derivatives were recorded using a Bruker D8 Eco Advanced diffractometer with a LYNXEYE XE-T detector and a generator with a Cu anode (radiation Cu Kα = 1.54 Å) operating at 40 kV and 25 mA. Measurements were carried out dispersing samples over glass sample holders (without further manipulation) and recording XRD patterns from 5 to 50° (2θ), with a step size of 0.02° and 1 s per step. Diffractograms were analyzed using a Diffrac Plus Eva software.

Molecular modeling methodology

The calculations were performed on Dell Precision 380 and SGI Virtu VS100 workstations, provided with the Discovery Studio v2.5 suite or the MOE2022.02 software package, respectively. The three-dimensional models of the studied compounds were constructed using template models of NSAIDs obtained from Cambridge Structural Database [53] (CSD System version 5.43; search and information retrieval with ConQuest [54] v2022.2.0). Therefore, models for the ASA, Salic, Ind, Nap, Ket, and Ibup derivatives were obtained from ACSALA29 [55], SALIAC [56], COYRUD [57], INDMET [58], KEMRUP [59], and JEKNOC10 [60] references, respectively.

The reference models (cell unit) were imported in the Discovery Studio v2.5 suite (DSv2.5) workspace and were constructed in gas phase under the Dreiding force field [61]. The most relevant non-bonded interactions were detected. These initial models were analyzed and further modified to the Se-NSAID compounds by means of the DSv2.5 *Builder* module. A first energy minimization was carried out by applying the Clean Geometry protocol (a fast, Dreiding-like force field [62]) to optimize the geometry of selected structures. The optimized theoretical cell structures were imported on the MOE2022.02 [63] workspace and minimized again with the implemented MOPAC engine (PM3 semi-empirical approach [64]). The most relevant interactions were obtained and analyzed from the final theoretical constructed cells.

Chromatography

Chromatographic studies were carried out for both compounds based on Nap-containing selenoesters with nitrile groups (**I.3d** and **I.3e**) to evaluate the stability of the different polymorphic forms under stress conditions. An HPLC/UV-DAD (HP 1100, Agilent Technologies, Santa Clara, CA, USA) equipped with a C18 column (Gemini 110A, 100×4.6 mm, 5 μm) from Phenomenex (Phenomenex, Torrance, CA, USA) was used. The mobile phase was a mixture of acetonitrile/water (50:50, *v/v*) for all the compounds

tested. The injection volume was 10 μL and the flow rate was 1 mL min $^{-1}$. UV-DAD detection was established at $\lambda = 254$ nm.

The stability assessment was performed in forced degradation conditions, using acid (HCl 1 M), alkaline (NaOH 0.1 M) or oxidative (H$_2$O$_2$ 3% *w/v*) media. Working solutions at 0.5 mg mL^{-1} in an acetonitrile/water mixture (50:50, *v/v*) of **I.3d** and **I.3e** (both Forms I and II) were prepared by diluting 100 μL of a stock solution for each compound in acetonitrile at a concentration of 1 mg mL^{-1} with 100 μL of the corresponding aqueous media for each condition. Data were recorded after different exposure times (0, 2, 6, 10, 18, 24, 48, and 72 h).

Cell culture conditions

The cell lines were obtained from the American Type Culture Collection (ATCC). Colon (HT-29), lung (HTB-54), and prostate (DU-145) cancer cell lines were maintained in RPMI 1640 medium (Gibco), supplemented with 10% fetal bovine serum (FBS; Gibco) and 1% antibiotics (10.00 units mL^{-1} penicillin and 10.00 mg mL^{-1} streptomycin; Gibco). Cells were preserved in tissue culture flasks at 37 °C and 5% CO$_2$. Culture medium was replaced every three days.

Cell viability assay

For each cell line, a total of 1×10^4 cells were seeded in 96-well plates and incubated at 37 °C and 5% CO$_2$ for 24 h. Compounds were dissolved in DMSO at a concentration of 0.01 M and serial dilutions were prepared. Cells were then treated with either DMSO or seven increasing concentrations ranging between 0.5 and 100 μM of the corresponding Se-NSAID derivative for 48 h. The effect of the isolated polymorphs of compounds **I.3d** and **I.3e** on cell viability was evaluated by the (3-(4,5-dimethylthiazol-2-yl)-2,5-diphenyltetrazolium bromide) (MTT) assay [65]. Briefly, a volume of 20 μL of MTT (5 mg mL^{-1}) was added to each well 2.5 h prior to experiment termination. At the end of the incubation, the medium was removed, and the formazan crystals formed by mitochondrial reduction of MTT were dissolved in 50 μL of DMSO. Cell viability was expressed as the half maximal inhibitory concentration (IC$_{50}$) values calculated from the absorbance measured at 550 nm on a microplate reader.

Statistical analysis

Biological data were expressed as the mean $\pm$ SD (standard deviation) and recorded from three independent experiments performed in triplicates. The IC$_{50}$ values were obtained by nonlinear curve regression analysis calculated by Origin-Pro 9.0. software. An unpaired *t* test ($P < 0.05$) was used to calculate the statistical significance of differences by comparing the IC$_{50}$ values between polymorphs of the same compound. Data were analyzed using GraphPad Prism version 8.0.1.

Results and discussion

Thermal characterization of the Se-NSAID derivatives

Thermal stability

The Se-NSAID derivatives were first subjected to calorimetric and thermogravimetric analyses to assess their thermal stability. The fusion and degradation temperatures (as T_{onset}) obtained are summarized for selenoesters of series I in Table 1, and for diacyl diselenides of series II in Table 2 (see DSC and TG curves in supplementary material). In general, compounds were found to show high temperatures, thus proving the relatively high stability of the Se-NSAID derivatives studied. The modeling data obtained have helped us to explain the high stability shown by these structures, once analyzed their conformational behavior and obtained the lowest energy conformation, since it has been possible to detect, through these studies, the establishment of the corresponding interactions that could enhance the inter- and intramolecular interactions in theoretical crystal cells.

Thus, and as shown in Fig. 2, the structural modifications involved in the design of the Se-NSAID compounds implied the introduction of a Se(C=O) group that increased the length of the main side chain and the conformational freedom, by introducing both a hydrogen bond acceptor (C=O) and a Se atom. The inclusion of these moieties could enhance the inter- and intramolecular interactions in theoretical crystal cells (Fig. 2), and the availability of empty *d* orbitals in the Se atom would facilitate these interactions [66]. Both of them would explain the high thermal stability of these compounds.

Remarkably, compounds based on an Ind core (**I.4a**, **I.4b**, **I.4c**, **I.4d**, **I.4e**, and **II.2**) presented the highest degradation temperatures observed overall. Interestingly, as shown in Fig. 3a for derivative **I.4a**, these compounds showed notable intermolecular pi–pi stacked interactions established between the indole rings, reinforced in some compounds by those formed between the chloro-benzene rings that decorated these derivatives. The presence of the methoxy moiety could also enhance the electronic dotation of this structural core. The resulting delocalization would reinforce the aforementioned interaction, which may explain the greater thermal stability shown by these NSAID derivatives containing an Ind structure.

Table 1 Thermal data for the degradation and fusion processes obtained for selenoesters of series I and the associated behavior

Ref	Scan	Fusion process (DSC)		Degradation process (TG)	Behavior
		T_{onset}/°C	ΔH_f /J g^{-1}	T_{onset}/°C	
I.1a	1st	94.1	104.6	152.7	III
	2nd	92.4	101.7		
	3rd	92.4	99.3		
I.2a	1st	112.7	86.3	154.5	III
	2nd	113.9	81.2		
	3rd	118.8	86.6		
I.3a	1st	88.6	60.1	221.0	II
	2nd	–	–		
I.4a	1st	161.5	81.6	230.1	II
	2nd	–	–		
I.5a	1st	53.2	41.7	191.1	II
	2nd	–	–		
I.1b*	1st	–	–	223.0	0
	2nd	–	–		
I.2b	1st	57.1	93.9	190.3	II
	2nd	–	–		
I.3b	1st	37.2	60.0	268.5	II
	2nd	–	–		
I.4b	1st	64.0	54.9	268.9	II
	2nd	–	–		
I.5b*	1st	–	–	282.0	0
	2nd	–	–		
I.1c	1st	112.9	103.7	164.9	III
	2nd	108.3	103.6		
	3rd	108.5	97.5		
I.2c	1st	90.4	47.7	177.0	III
	2nd	85.2	61.1		
I.3c	1st	71.9	52.6	220.2	II
	2nd	–	–		
I.4c	1st	94.2	39.9	247.3	II
	2nd	–	–		
I.5c*	1st	–	–	240.0	0
	2nd	–	–		
I.1d	1st	61.2	101.1	227.1	III
	2nd	60.3	79.4		
I.2d	1st	55.6	41.4	130.4	II
	2nd	–	–		
I.3d	1st	71.3	89.8	251.8	IV
	2nd	49.3	57.6		
	3rd	47.0	54.2		
I.4d	1st	–	–	259.6	I
	2nd	–	–		
I.5d	1st	58.6	82.8	252.0	III
	2nd	56.6	75.3		
I.1e	1st	42.5	69.2	218.6	III
	2nd	41.2	64.1		

Table 1 (continued)

Ref	Scan	Fusion process (DSC)		Degradation process (TG)	Behavior
		T_{onset}/°C	ΔH_f /J g^{-1}	T_{onset}/°C	
I.2e	1st	84.0	98.1	190.8	III
	2nd	82.2	97.6		
I.3e	1st	68.8	83.4	266.7	IV
	2nd	50.6	62.0		
I.4e	1st	102.2	75.3	271.2	II
	2nd	–	–		
I.5e	1st	50.2	68.0	254.2	III
	2nd	50.0	56.7		

*Compound is liquid at room temperature

Table 2 Thermal data for the degradation and fusion processes obtained for diacyl diselenides of series II and the associated behavior

Ref	Scan	Fusion process (DSC)		Degradation process (TG)	Behavior
		T_{onset}/°C	ΔH_f /J g^{-1}	T_{onset}/°C	
II.1	1st	62.4	35.7	225.0	II
	2nd	–	–		
II.2	1st	91.3	40.6	240.1	IV
	2nd	47.9	7.4		
	3rd	46.4	6.6		
II.3	1st	113.8	65.8	224.8	II
	2nd	–	–		
II.4	1st	54.0	44.6	239.2	II
	2nd	–	–		
II.5*	1st	–	–	243.4	0
	2nd	–	–		

*Compound is liquid at room temperature

Besides, the establishment of strong pi–pi stacked interactions that could contribute to the stabilization (Fig. 3) can also be suggested for Nap derivatives (**I.3a**, **I.3b**, **I.3c**, **I.3d**, **I.3e**, and **II.3**) which presented also high degradation temperatures (Tables 1 and 2). In these cases, the presence of the planar naphthalene ring attached to a methoxy moiety that strengthened the electronic delocalization could increase the possibility of generating resonance hybrids and intermolecular interactions.

On the other hand, no relationships could be elucidated among the different substituents attached to the selenoester moiety (Fig. 1a) and their thermal stability on the decomposition (Table 1). The influence that the different decorations introduced on the selenoester moiety may have on the thermal stability seemed not to be clearly established by molecular modeling studies. In this context, as shown in Fig. 3c–d, a decrease in the established interactions was

Fig. 2 Representative examples of interactions mediated by the Se(C=O) moiety detected for compounds **I.1a**, **1.2a** and **II.1** (interactions in light blue dotted line; C in dark gray; H in light gray; O in red; Se in orange)

I.1a

I.2a

II.1

(a) I.4a   **(b)** I.3a   **(c)** I.3d   **(d)** I.3e

(e) II.1   **(f)** I.1a   **(g)** II.3
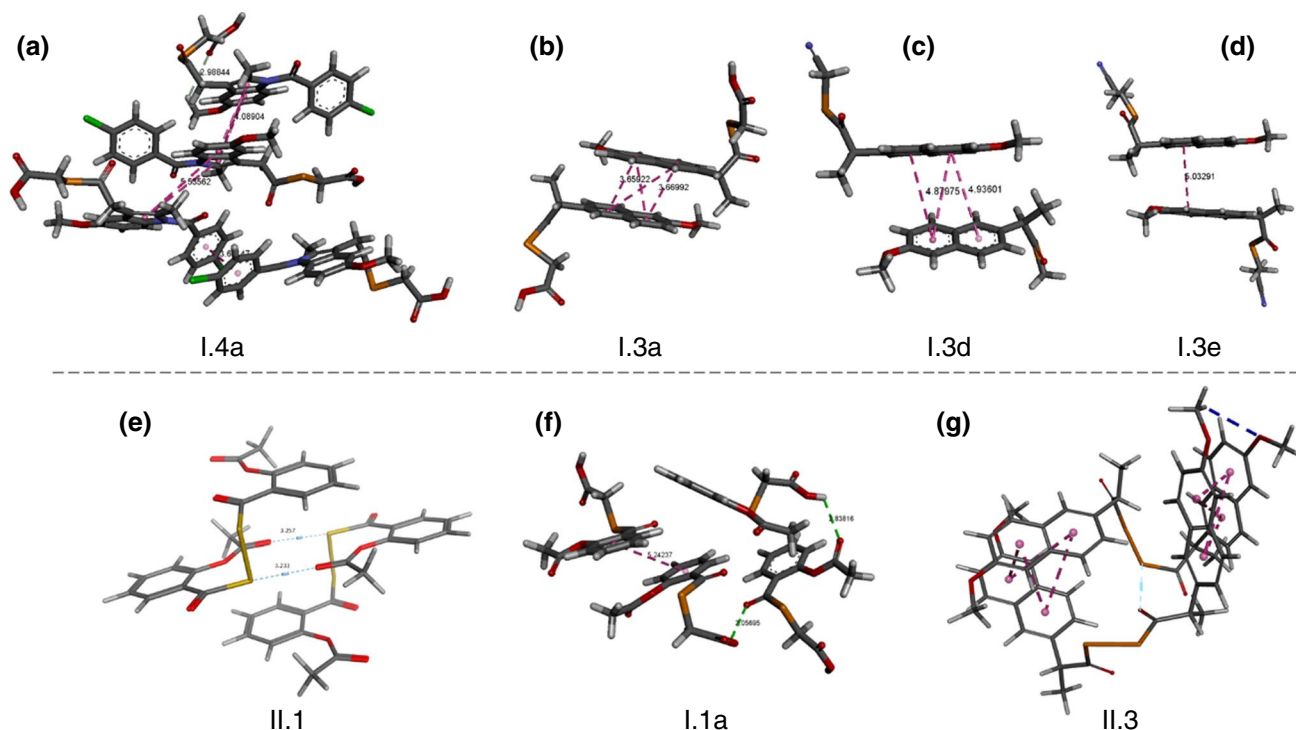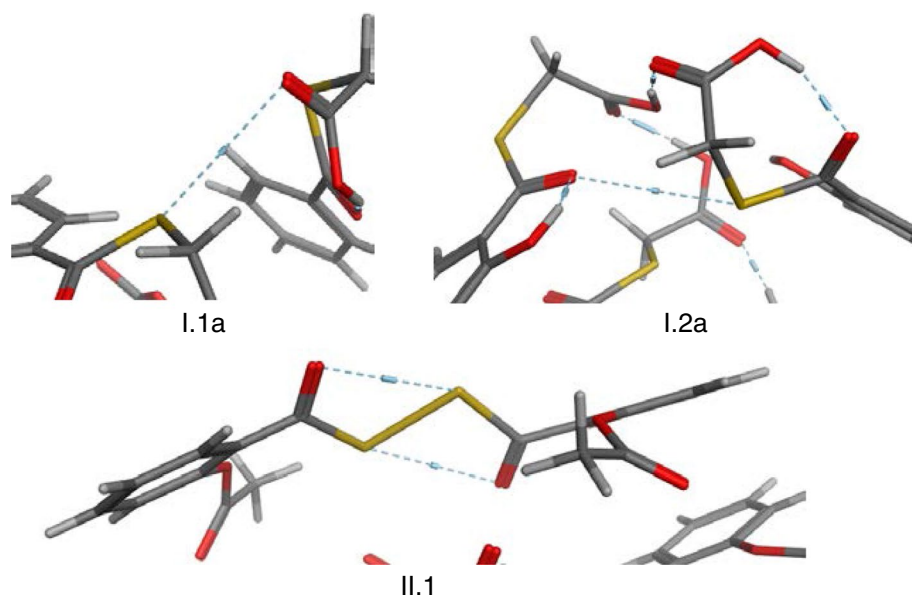
Fig. 3 Examples of modeled compounds showing their most relevant interactions: **a** compound **I.4a**, **b** compound **I.3a**, **c** compound **I.3d**, **d** compound **I.3e**, **e** compound **II.1**, **f** compound **I.1a**, **g** compound **II.3** (dark purple lines: pi–pi stacked; light purple lines: pi-alkyl interac-tion and hydrophobic interaction; dark blue lines: carbon-hydrogen bond interaction; green and light blue lines: hydrogen bond; distances in Å; C in dark gray; H in light gray; O in red; N in blue; Se in orange; Cl in green)

observed only for derivatives **I.3d** and **I.3e**, which incorporated a nitrile group. In fact, the four pi–pi interactions detected for compound **I.3a** (Fig. 3b) were weakened in the other derivatives of this group as the distance between

the naphthalene rings increased, reaching only one interaction in derivative **I.3e** (Fig. 3d).

The thermal stability could also be affected by molecular symmetry. In this context, NSAID derivatives of series

II based on a diacyl diselenide (Table 2) showed relatively high stability, since all the compounds presented degradation temperatures above 220 °C. As showed in other studies [16, 67], symmetric molecules such as compounds belonging to series II (Fig. 1b) could tend to form more packageable arrangements, leading to an increase in the thermal stability. In fact, as shown in Fig. 3e with compound **II.1** as a representative example, the theoretical proposal of a dimeric model showed the intermolecular interactions established between the Se atoms and the oxo moieties, in which unshared electron pairs from oxygen can interact with Se orbitals as previously described.

The Se-NSAID derivatives were then analyzed by DSC and subjected to successive cycles of melting and recrystallization. Calorimetric measurements were carried out by heating the samples up to temperatures 20 °C below the T_{onset} of the degradation process obtained by TG analysis. The results expressed as the fusion temperature (T_{onset}) and the enthalpy of fusion (ΔH_f) are outlined in Tables 1 and 2 for both series of compounds. Derivatives that were liquid at room temperature or in an initial amorphous state were excluded from this study.

Hence, analysis of the calorimetric data revealed some interesting considerations regarding the stability of the crystalline form of the compounds. For instance, among the substituents linked to the selenoester group in series I, the compounds including a carboxylic acid group (compounds **I.1-5a**) presented in general the highest values of fusion temperatures (Table 1). These data could suggest the possible formation of intermolecular hydrogen bonds, as can be seen in Fig. 3f for derivative **I.1a** as a representative example. Hydrogen bonds can establish stronger interactions than other dipole–dipole attractions, and so the presence of a chemical group that could enable such intermolecular bonds would allow more compact and rigid crystalline structures, thus enhancing their fusion temperature [67].

In this context, the highest fusion temperature of series I (Table 1) was observed for compound **I.4a**, suggesting that its higher thermal stability could be the result of both the aforementioned resonance effect induced by the Ind structure (electronic delocalization) and intermolecular interactions (Fig. 3a). On the contrary, although the formation of hydrogen bonds could also be suggested for ester and amide groups (compounds **I.1-5b** and **I.1-5c**), the fusion temperatures did not show any particular tendency in this regard. Likewise, no differences were observed for compounds including a nitrile group (compounds **I.1-5d** and **I.1-5e**) concerning their thermal stability.

Furthermore, the Nap derivative **II.3** presented the highest fusion temperature among the diacyl diselenides of series II (Table 2). The explanation for such behavior could be also related to the molecular symmetry, since a framework of pi–pi stacked and hydrogen bond intermolecular

interactions, analogous to compound **I.4a**, was detected by the molecular modeling analysis carried out for this compound (Fig. 3g compared to **3a**).

Classification and identification of polymorphism

To establish possible polymorphic behaviors, samples of all compounds were subjected to consecutive cycles of melting and recrystallization by DSC, as discussed in the previous section. The identification of polymorphism was also confirmed by XRD analysis. Thus, compounds were classified according to five different calorimetric behaviors.

- *Behavior 0*: Compounds that were in a liquid state at room temperature, and therefore, no T_{onset} of the fusion process could be obtained for these derivatives. These compounds (**I.1b**, **I.5b**, **I.5c**, and **II.5**) are marked with an asterisk in Tables 1 and 2.
- *Behavior I*: A compound that did not show any fusion process at the range of temperatures studied, so the compound was originally in an amorphous solid state and did not transit into another form after successive cycles. This behavior was displayed by Ind derivative **I.4d**. The absence of a crystalline form was also corroborated by XRD, as shown in the diffractogram for compound **I.4d** in Fig. 4. Interestingly, only this Ind-derived compound was amorphous originally. In this case, the presence of such a voluminous scaffold as the Ind core may hinder the packaging of the molecule into a crystalline pattern, thus adopting an amorphous state.

Behavior II: Compounds that were initially in a crystalline form and after a first melting-cooling scan showed a phase transition into an amorphous or mainly amorphous state. The Se-NSAID derivatives that followed this behavior
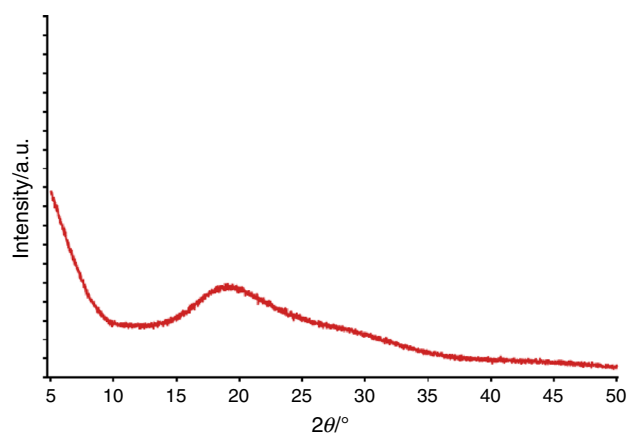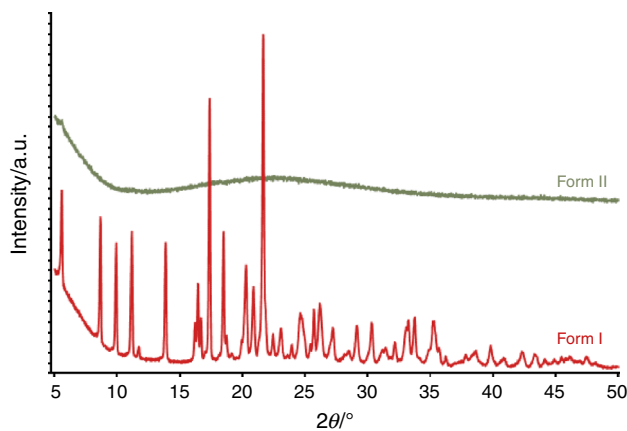

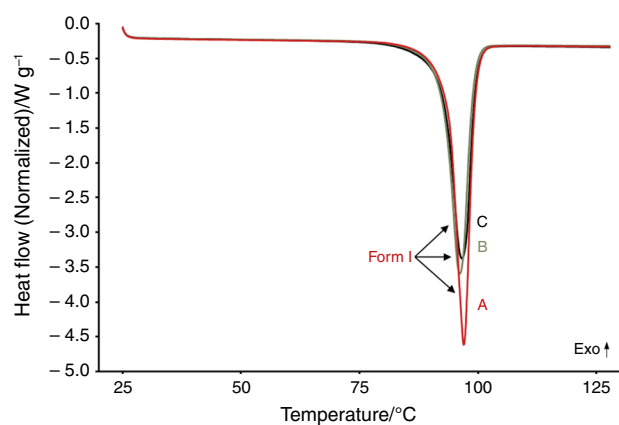**Fig. 4** X-ray diffractogram of compound **I.4d** (as representative example of behavior I)
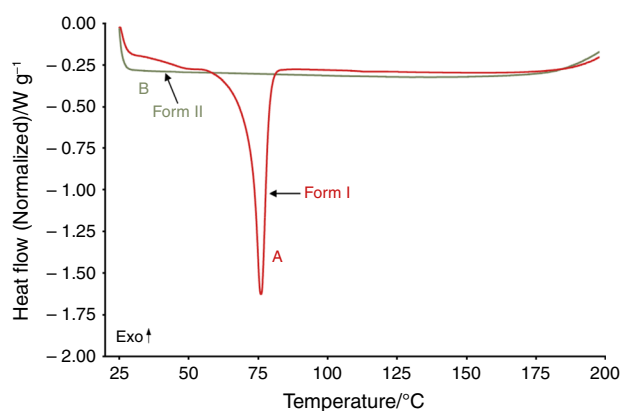
Fig. 5 DSC curves of compound **I.3c** (as representative example of behavior II). Red line, curve A: first scan; gray line, curve B: second scan after a cycle of heating/cooling/heating
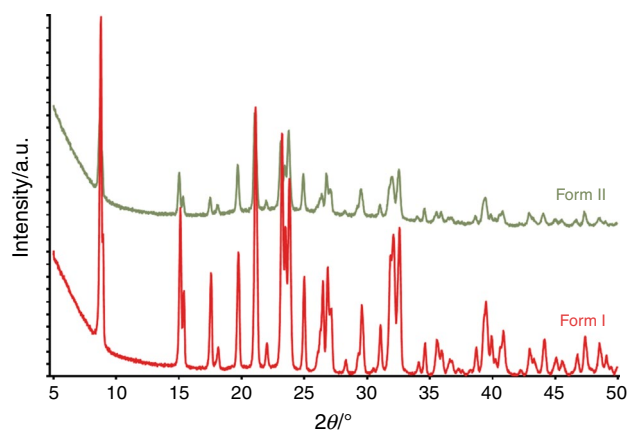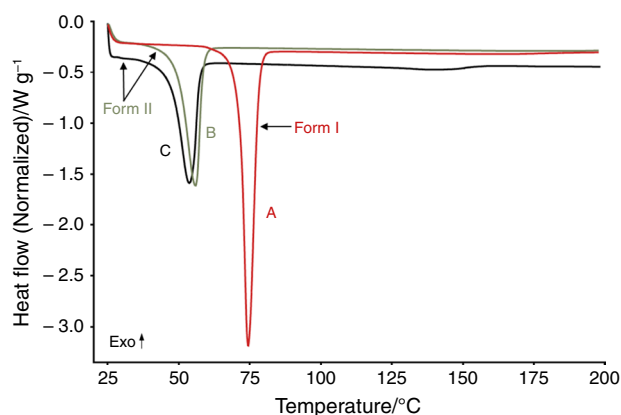

Fig. 7 DSC curves of compound **I.1a** (as representative example of behavior III). Red line, curve A: first scan; gray line, curve B: second scan after a cycle of heating/cooling/heating; black line, curve C: third scan after cycles of heating/cooling/heating

Fig. 6 X-ray diffractogram of compound **I.3c** (as representative example of behavior II). Red line: original form (Form I); gray line: amorphous solid form (Form II) after a melting-cooling scan
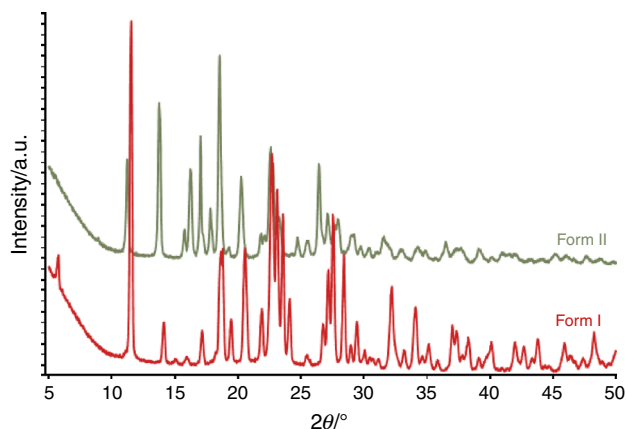

Fig. 8 X-ray diffractogram of compound **I.1a** (as representative example of behavior III). Red line: original form (Form I); gray line: same crystalline form (Form I) after a melting-cooling scan

were **I.3a**, **I.4a**, **I.5a**, **I.2b**, **I.3b**, **I.4b**, **I.3c**, **I.4c**, **I.2d**, **I.4e**, **II.1**, **II.3**, and **II.4** (supplementary material). This polymorphic behavior was observed by DSC curves and XRD patterns, as shown in Figs. 5 and 6, respectively, for compound **I.3c**, as an example. Thus, an endothermic melting process was recorded in the first scan, whereas no fusion process was observed by DSC after the second scan due to the transition into an amorphous phase. The complete curve (Fig. 5) also showed that other processes at higher or lower temperatures could be excluded. Likewise, degradation processes were also discarded through the parallel DSC and TG analysis. Additionally, the XRD patterns collected before and after heating the samples showed the absence of the initial crystalline phase (denoted as Form I in Fig. 6) after the first scan.

Behavior III: Compounds that displayed an initial crystalline form that was not altered after the melting-recrystallization cycle, and thus no evidence of polymorphism

could be ascribed to these derivatives. The compounds that showed this type of behavior were derivatives **I.1a**, **I.2a**, **I.1c**, **I.2c**, **I.1d**, **I.5d**, **I.1e**, **I.2e**, and **I.5e** (supplementary material). The endothermic melting process observed in the first thermal scan remained after successive cooling-heating cycles, as shown in Fig. 7 for compound **I.1a**, as an example. The recrystallization into the same form after cooling was also confirmed by XRD (Fig. 8), since no changes were found in the position of the peaks when comparing the original diffractogram with the data recorded after the thermal treatment.

Behavior IV: Compounds that showed recrystallization into a new polymorphic form with a T_{onset} lower than the endothermic process measured at the first melting-recrystallization scan. In successive cycles, the new polymorph maintained its crystalline form. The compounds

Fig. 9 DSC curves of compound **I.3d** (as representative example of behavior IV). Red line, curve A: first scan; gray line, curve B: second scan after a cycle of heating/cooling/heating; black line, curve C: third scan after cycles of heating/cooling/heating

Fig. 10 X-ray diffractogram of compound **I.3d** (as representative example of behavior IV). Red line: original polymorph (Form I); gray line: new polymorph (Form II) after a melting-cooling scan

that showed this polymorphic behavior were derivatives **I.3d**, **I.3e**, and **II.2** (supplementary material). As shown in Fig. 9 for the representative compound **I.3d,** as an example, initially an endothermic process was observed for the original form (in red, Form I), but another endothermic process was discerned in a second scan at a lower temperature that corresponded to a new crystalline polymorph (in gray, Form II) that was not altered in subsequent cycles. Likewise, the two polymorphic forms were also confirmed by XRD. As displayed in Fig. 10, the XRD patterns of compound **I.3d** showed different positions of the peaks, corresponding to unequivocally distinct crystalline phases.

Stability of the polymorphic forms of compounds I.3d and I.3e under stress conditions

Compounds classified within behavior IV in the previous section according to the DSC and XRD data were then exposed to acid hydrolysis (HCl 1 M), basic hydrolysis (NaOH 0.1 M), and oxidation (H$_2$O$_2$ 3% *w/v*) to test the stability of the different polymorphic forms under certain stress conditions. Compound **II.2** was discarded for this study given that it was the only compound described with this behavior that was previously found to be completely inactive toward cancer cells. Thus, the stability of the crystalline polymorphs of compounds **I.3d** and **I.3e** subjected to the different treatments was analyzed at several time points along 72 h using HPLC/UV-DAD.

As shown in Fig. 11, no apparent differences were detected among the polymorphic forms of the two Se-NSAID derivatives. Furthermore, both compounds showed a similar stability profile when subjected to the three conditions tested. Thus, **I.3d** and **I.3e** were found to be stable under an acid medium for 48 h, whereas a slight degradation could be observed by the end of the experiment at longer times. On the contrary, the Se-NSAID derivatives underwent a rapid and complete degradation under alkaline conditions, as both polymorphic forms of the two compounds were drastically degraded after 2 h of exposure to NaOH medium. Notably, compounds showed a clear degradation over time under oxidative conditions, although not as pronounced as in the alkaline medium. Herein, the polymorphs of derivative **I.3d** were slightly more stable than those of derivative **I.3e**, since the latter were completely degraded after 48 h of exposure to H$_2$O$_2$ medium. Concurrently, degradation product peaks were also detected under both alkaline and oxidative conditions.

Effect of polymorphism on the cytotoxicity of Se-NSAID derivatives

The effect of the different polymorphic forms of compounds **I.3d** and **I.3e** on the cell viability was assessed against three cancer cell lines using the MTT assay described in the Experimental section. Cells were exposed to seven increasing concentrations of both crystalline polymorphic forms (Forms I and II) of each compound for 48 h. The results are expressed as the IC$_{50}$ values and are outlined in Table 3.

As shown in Table 3, the original Form I of compounds **I.3d** and **I.3e** containing a Nap scaffold modified by the inclusion of Se as a selenoester group and different nitrile functionalities displayed potent cytotoxic activity, as previously reported [48]. Hence, the IC$_{50}$ values were lower than 7 μM in all the cancer cell lines tested. Interestingly, the other isolated crystalline form (Form II) did not show any significant difference with respect to their corresponding
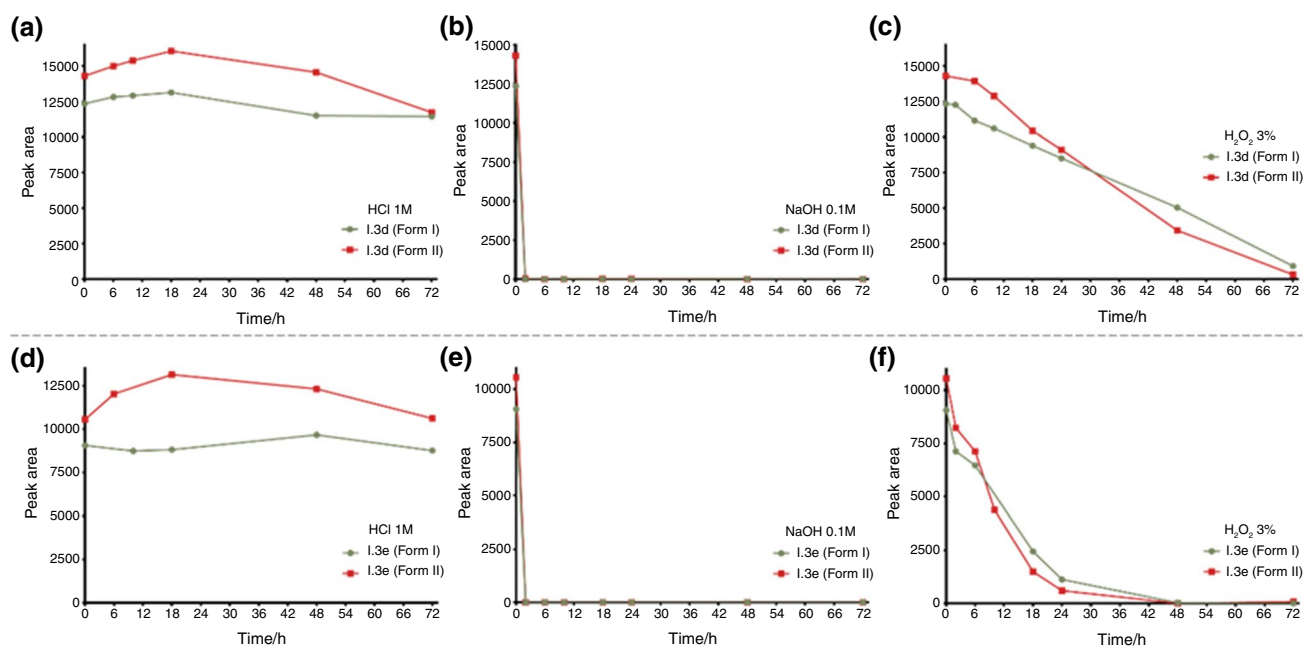
Fig. 11 Stability of crystalline polymorphs of Se-NSAID derivatives along 72 h under stress conditions: **a** acid medium for compound I.3d (Form I and Form II), **b** alkaline medium for compound I.3d (Form I and Form II), **c** oxidative medium for compound I.3d (Form I and Form II), **d** acid medium for compound I.3e (Form I and Form II), **e** alkaline medium for compound I.3e (Form I and Form II), **f** oxidative medium for compound I.3e (Form I and Form II)

Table 3 Antiproliferative activity of the Se-NSAID compounds expressed as IC_{50} values ((mean ± SD) µM) in colon (HT-29), lung (HTB-54), and prostate (DU-145) cancer cell lines

Compounds	Colon cells HT-29	Lung cells HTB-54	Prostate cells DU-145
I.3d (Form I)	2.6 ± 0.6	6.2 ± 1.0	3.6 ± 0.2
I.3d (Form II)	2.8 ± 0.4	6.2 ± 0.2	3.4 ± 0.2
I.3e (Form I)	8.0 ± 1.1	6.0 ± 0.9	4.0 ± 0.2
I.3e (Form II)	6.6 ± 2.2	5.8 ± 1.0	3.9 ± 0.2

original polymorph. Thus, for selenoester compounds **I.3d** and **I.3e**, both crystalline forms displayed similar cytotoxicity toward cancer cells. This behavior in the biological activity should be taken into account in the development of this type of NSAID derivatives.

Conclusions

Preliminary studies on thermal characterization are of great importance for detecting and isolating possible polymorphic forms and thus optimizing the crystallization process in drug development. In this study, the thermal characterization and identification of potential polymorphic forms of thirty Se-NSAID derivatives were carried out with a combination of TG, DSC, and XRD techniques. Overall, compounds tended

to show high stability in the decomposition process, Ind- and Nap-containing derivatives having the highest degradation temperatures observed. The thermal stability of such compounds could be conditioned by the establishment of resonance structures that enhance the electronic delocalization within the aromatic rings, allowing strong pi–pi stacked interactions as determined by molecular modeling studies. The molecular symmetry of the Se-NSAID based on a diacyl diselenide (series II) could also be considered as another factor for their increased thermal stability, due to boosting a more packageable arrangement in the spatial disposition. Likewise, for derivatives containing a carboxylic acid group in series I, the enhancement observed in their values of fusion temperatures could be related to the feasible formation of hydrogen bonds.

Compounds were also classified according to five different behaviors based on their thermal behavior. Among the thirty Se-NSAID derivatives, compounds **I.3d**, **I.3e** (Nap-containing derivatives), and **II.2** (an Ind-containing derivative) were found to present two different crystalline polymorphs. Additionally, the stability study of **I.3d** and **I.3e** under acid, alkaline or oxidative stress conditions showed a prominent degradation under basic and oxidative hydrolysis over time, without differences among the polymorphic forms.

Furthermore, to test the possible variation in the cytotoxic activity of the Se-NSAID derivatives depending on the polymorphs, the two isolated crystalline forms of compounds

I.3d and **I.3e** were screened against colon, lung, and prostate cancer cell lines. Interestingly, no significant differences were observed among the distinct forms of each compound, thus proving that for this type of Se-NSAID derivatives, polymorphism was not a determinant factor in the therapeutic effect.

Declarations

Conflict of interest The authors declare no conflict of interest.

References

1. Pindelska E, Sokal A, Kolodziejski W. Pharmaceutical cocrystals, salts and polymorphs: advanced characterization techniques. Adv Drug Deliv Rev. 2017;117:111–46. https://doi.org/10.1016/j.addr.2017.09.014.
2. Karagianni A, Malamatari M, Kachrimanis K. Pharmaceutical cocrystals: new solid phase modification approaches for the formulation of APIs. Pharmaceutics. 2018;10:18. https://doi.org/10.3390/pharmaceutics10010018.
3. Lee AY, Erdemir D, Myerson AS. Crystal polymorphism in chemical process development. Annu Rev Chem Biomol Eng. 2011;2:259–80. https://doi.org/10.1146/annurev-chembioeng-061010-114224.
4. Chadha R, Haneef J. Near-infrared spectroscopy: effective tool for screening of polymorphs in pharmaceuticals. Appl Spectrosc Rev. 2015;50:565–83. https://doi.org/10.1080/05704928.2015.1044663.
5. Higashi K, Ueda K, Moribe K. Recent progress of structural study of polymorphic pharmaceutical drugs. Adv Drug Deliv Rev. 2017;117:71–85. https://doi.org/10.1016/j.addr.2016.12.001.
6. Shi Q, Chen HB, Wang YA, Xu J, Liu ZY, Zhang C. Recent advances in drug polymorphs: aspects of pharmaceutical properties and selective crystallization. Int J Pharm. 2022;611: 121320. https://doi.org/10.1016/j.ijpharm.2021.121320.
7. Knapman K. Polymorphic predictions: understanding the nature of crystalline compounds can be critical in drug development and manufacture. Mod Drug Discov. 2000;3(53–54):57.
8. ICH. ICH Topic Q 6 A Specifications: test procedures and acceptance criteria for new drug substances and new drug products: chemical substances. In: Int conf harmon tech requir regist pharm hum use. 1999.
9. Rodríguez-Spong B, Price CP, Jayasankar A, Matzger AJ, Rodríguez-Hornedo N. General principles of pharmaceutical solid polymorphism: a supramolecular perspective. Adv Drug Deliv Rev. 2004;56:241–74. https://doi.org/10.1016/j.addr.2003.10.005.
10. Bruylants G, Wouters J, Michaux C. Differential scanning calorimetry in life science: thermodynamics, stability, molecular recognition and application in drug design. Curr Med Chem. 2005;12:2011–20. https://doi.org/10.2174/0929867054546564.
11. Baird JA, Taylor LS. Evaluation of amorphous solid dispersion properties using thermal analysis techniques. Adv Drug Deliv Rev. 2012;64:396–421. https://doi.org/10.1016/j.addr.2011.07.009.
12. Ma XY, Williams RO. Characterization of amorphous solid dispersions: an update. J Drug Deliv Sci Technol. 2019;50:113–24. https://doi.org/10.1016/j.jddst.2019.01.017.
13. Di Martino P, Magnoni F, Peregrina DV, Gigliobianco MR, Censi R, Malaj L. Formation, physicochemical characterization, and thermodynamic stability of the amorphous state of drugs and excipients. Curr Pharm Des. 2016;22:4959–74. https://doi.org/10.2174/1381612822666160726105658.
14. Thakral NK, Zanon RL, Kelly RC, Thakral S. Applications of powder X-ray diffraction in small molecule pharmaceuticals: achievements and aspirations. J Pharm Sci. 2018;107:2969–82. https://doi.org/10.1016/j.xphs.2018.08.010.
15. Benmore CJ, Benmore SR, Edwards AD, Shrader CD, Bhat MH, Cherry BR, et al. A high energy X-ray diffraction study of amorphous indomethacin. J Pharm Sci. 2022;111:818–24. https://doi.org/10.1016/j.xphs.2021.12.003.
16. Etxebeste M, Durán A, Sanmartín C, González-Penas E, Plano D, Lizarraga E. Thermal characterization and stability evaluation of leishmanicidal selenocyanate and diselenide derivatives. J Therm Anal Calorim. 2022;147:3127–39. https://doi.org/10.1007/s10973-020-10544-x.
17. Alcolea V, Garnica P, Palop JA, Sanmartín C, González-Penas E, Durán A, et al. Antitumoural sulphur and selenium heteroaryl compounds: thermal characterization and stability evaluation. Molecules. 2017;22:1314. https://doi.org/10.3390/molecules22081314.
18. Rao PNP, Knaus EE. Evolution of nonsteroidal anti-inflammatory drugs (NSAIDs): cyclooxygenase (COX) inhibition and beyond. J Pharm Pharm Sci. 2008;11:81–110. https://doi.org/10.18433/j3t886.
19. Lichtenberger LM, Fang DX, Bick RJ, Poindexter BJ, Phan T, Bergeron AL, et al. Unlocking aspirin's chemopreventive activity: role of irreversibly inhibiting platelet cyclooxygenase-1. Cancer

Prev Res (Phila). 2017;10:142–52. https://doi.org/10.1158/1940-6207.CAPR-16-0241.

20. Ma SD, Guo CJ, Sun CY, Han TT, Zhang HM, Qu GB, et al. Aspirin use and risk of breast cancer: a meta-analysis of observational studies from 1989 to 2019. Clin Breast Cancer. 2021;21:552–65. https://doi.org/10.1016/j.clbc.2021.02.005.

21. Mohammed A, Yarla NS, Madka V, Rao CV. Clinically relevant anti-inflammatory agents for chemoprevention of colorectal cancer: new perspectives. Int J Mol Sci. 2018;19:2332. https://doi.org/10.3390/ijms19082332.

22. Figueiredo JC, Jacobs EJ, Newton CC, Guinter MA, Cance WG, Campbell PT. Associations of aspirin and non-aspirin non-steroidal anti-inflammatory drugs with colorectal cancer mortality after diagnosis. J Natl Cancer Inst. 2021;113:833–40. https://doi.org/10.1093/jnci/djab008.

23. Hung CH, Lin YC, Chang YH, Lin YC, Huang HY, Yeh WJ, et al. The effect of NSAIDs exposure on breast cancer risk in female patients with autoimmune diseases. Eur J Cancer Prev. 2019;28:428–34. https://doi.org/10.1097/CEJ.0000000000000476.

24. Scheiman JM. NSAID-induced gastrointestinal injury. A focused update for clinicians. J Clin Gastroenterol. 2016;50:5–10. https://doi.org/10.1097/MCG.0000000000000432.

25. Gurbel P, Tantry U, Weisman S. A narrative review of the cardiovascular risks associated with concomitant aspirin and NSAID use. J Thromb Thrombolysis. 2019;47:16–30. https://doi.org/10.1007/s11239-018-1764-5.

26. Ramos-Inza S, Ruberte AC, Sanmartín C, Sharma AK, Plano D. NSAIDs: old acquaintance in the pipeline for cancer treatment and prevention-structural modulation, mechanisms of action, and bright future. J Med Chem. 2021;64:16380–421. https://doi.org/10.1021/acs.jmedchem.1c01460.

27. Sanphui P, Bolla G, Nangia A. High solubility piperazine salts of the nonsteroidal anti-inflammatory drug (NSAID) meclofenamic acid. Cryst Growth Des. 2012;12:2023–36. https://doi.org/10.1021/cg300002p.

28. Tumanova N, Tumanov N, Fischer F, Morelle F, Ban V, Robeyns K, et al. Exploring polymorphism and stoichiometric diversity in naproxen/proline cocrystals. CrystEngComm. 2018;20:7308–21. https://doi.org/10.1039/c8ce01338a.

29. Liu H, Yang X, Wu SY, Zhang MT, Parkin S, Cao S, et al. An investigation of the polymorphism of a potent nonsteroidal anti-inflammatory drug flunixin. CrystEngComm. 2020;22:448–57. https://doi.org/10.1039/c9ce01619h.

30. López-Mejías V, Kampf JW, Matzger AJ. Nonamorphism in flufenamic acid and a new record for a polymorphic compound with solved structures. J Am Chem Soc. 2012;134:9872–5. https://doi.org/10.1021/ja302601f.

31. Sacchi P, Reutzel-Edens SM, Cruz-Cabeza AJ. The unexpected discovery of the ninth polymorph of tolfenamic acid. CrystEngComm. 2021;23:3636–47. https://doi.org/10.1039/d1ce00343g.

32. Raza K, Ratan S, Kumar M, Kumar P, Chaturvedi S, Katare OP. Aceclofenac polymorphs: preparation, characterization and intestinal permeation studies. J Drug Deliv Sci Technol. 2017;39:69–74. https://doi.org/10.1016/j.jddst.2017.03.004.

33. Li Q, Bond AD, Korter TM, Zeitler JA. New insights into the crystallographic disorder in the polymorphic forms of aspirin from low-frequency vibrational analysis. Mol Pharm. 2022;19:227–34. https://doi.org/10.1021/acs.molpharmaceut.1c00727.

34. Surwase SA, Boetker JP, Saville D, Boyd BJ, Gordon KC, Peltonen L, et al. Indomethacin: new polymorphs of an old drug. Mol Pharm. 2013;10:4472–80. https://doi.org/10.1021/mp400299a.

35. Zayed MA, Hawash MF, El-Desawy M, El-Gizouli AMM. Investigation of naproxen drug using mass spectrometry, thermal analyses and semi-empirical molecular orbital calculation. Arab

J Chem. 2017;10:351–9. https://doi.org/10.1016/j.arabjc.2013.09.025.

36. Caglar S, Altay A, Harurluoglu B, Yeniceri EKK, Caglar B, Sahin O. Synthesis, structural characterization and evaluation of anti-cancer activity of polymeric silver(I) complexes based on niflumic acid/naproxen and picoline derivatives. Coord Chem Rev. 2022;75:178–96. https://doi.org/10.1080/00958972.2022.2045586.

37. Pipkin LG, Copeland BC, Cojocaru OA. Liquid co-crystals of dual-active phenothiazine-NSAID drugs: synthesis, spectroscopic, and thermal characterization. ACS Omega. 2022;7:16990–7001. https://doi.org/10.1021/acsomega.1c07382.

38. Bannach G, Arcaro R, Ferroni DC, Siqueira AB, Treu O, Ionashiro M, et al. Thermoanalytical study of some anti-inflammatory analgesic agents. J Therm Anal Calorim. 2010;102:163–70. https://doi.org/10.1007/s10973-010-0939-x.

39. Medeiros RS, Ferreira APG, Cavalheiro ETG. Thermal behavior of naproxen and ketoprofen nonsteroidal anti-inflammatory drugs. J Therm Anal Calorim. 2020;142:849–59. https://doi.org/10.1007/s10973-020-09389-1.

40. Kim SJ, Choi MC, Park JM, Chung AS. Antitumor effects of selenium. Int J Mol Sci. 2021;22:11844. https://doi.org/10.3390/ijms222111844.

41. Chuai HY, Zhang SQ, Bai HR, Li JY, Wang Y, Sun JJ, et al. Small molecule selenium-containing compounds: recent development and therapeutic applications. Eur J Med Chem. 2021;223:113621. https://doi.org/10.1016/j.ejmech.2021.113621.

42. Radomska D, Czarnomysy R, Radomski D, Bielawski K. Selenium compounds as novel potential anticancer agents. Int J Mol Sci. 2021;22:1009. https://doi.org/10.3390/ijms22031009.

43. Gandin V, Khalkar P, Braude J, Fernandes AP. Organic selenium compounds as potential chemotherapeutic agents for improved cancer treatment. Free Radic Biol Med. 2018;127:80–97. https://doi.org/10.1016/j.freeradbiomed.2018.05.001.

44. Ruberte AC, Sanmartín C, Aydillo C, Sharma AK, Plano D. Development and therapeutic potential of selenazo compounds. J Med Chem. 2020;63:1473–89. https://doi.org/10.1021/acs.jmedchem.9b01152.

45. Zeng HW, Cheng WH, Johnson LK. Methylselenol, a selenium metabolite, modulates p53 pathway and inhibits the growth of colon cancer xenografts in Balb/c mice. J Nutr Biochem. 2013;24:776–80. https://doi.org/10.1016/j.jnutbio.2012.04.008.

46. Tan HW, Mo HY, Lau ATY, Xu YM. Selenium species: current status and potentials in cancer prevention and therapy. Int J Mol Sci. 2019;20:75. https://doi.org/10.3390/ijms20010075.

47. Sanmartín C, Plano D, Sharma AK, Palop JA. Selenium compounds, apoptosis and other types of cell death: an overview for cancer therapy. Int J Mol Sci. 2012;13:9649–72. https://doi.org/10.3390/ijms13089649.

48. Ramos-Inza S, Encío I, Raza A, Sharma AK, Sanmartín C, Plano D. Design, synthesis and anticancer evaluation of novel Se-NSAID hybrid molecules: Identification of a Se-indomethacin analog as a potential therapeutic for breast cancer. Eur J Med Chem. 2022;244:114839. https://doi.org/10.1016/j.ejmech.2022.114839.

49. Tanini D, D'Esopo V, Tatini D, Ambrosi M, Lo Nostro P, Capperucci A. Selenated and sulfurated analogues of triacyl glycerols: selective synthesis and structural characterization. Chem. 2020;26:2719–25. https://doi.org/10.1002/chem.201904686.

50. Díaz M, Palop JA, Sanmartín C, Lizarraga E. Thermal stability and decomposition of urea, thiourea and selenourea analogous diselenide derivatives. J Therm Anal Calorim. 2017;127:1663–74. https://doi.org/10.1007/s10973-016-5645-x.

51. Phadnis PP, Kunwar A, Kumar M, Mishra R, Wadawale A, Priyadarsini KI, et al. Study of polymorphism in 2, 2

'-diselenobis(3-pyridinol). J Organomet Chem. 2017;852:1–7. https://doi.org/10.1016/j.jorganchem.2017.09.029.

52. Plano D, Lizarraga E, Palop JA, Sanmartín C. Study of polymorphism of organosulfur and organoselenium compounds. J Therm Anal Calorim. 2011;105:1007–13. https://doi.org/10.1007/s10973-010-1012-5.

53. Groom CR, Bruno IJ, Lightfoot MP, Ward SC. The cambridge structural database. Acta Crystallogr B: Struct Sci Cryst Eng Mater. 2016;72:171–9. https://doi.org/10.1107/S2052520616003954.

54. Bruno IJ, Cole JC, Edgington PR, Kessler M, Macrae CF, McCabe P, et al. New software for searching the Cambridge structural database and visualizing crystal structures. Acta Crystallogr B: Struct Sci Cryst Eng Mater. 2002;58:389–97. https://doi.org/10.1107/s0108768102003324.

55. Matsumoto T, Yamano A, Sato T, Ferrara JD, White FJ, Meyer M. "What is this?" A structure analysis tool for rapid and automated solution of small molecule structures. J Chem Crystallogr. 2021;51:438–50. https://doi.org/10.1007/s10870-020-00867-w.

56. Sundaralingam M, Jensen LH. Refinement of the structure of salicylic acid. Acta Crystallogr. 1965;18:1053–8. https://doi.org/10.1107/s0365110x65002517.

57. Ravikumar K, Rajan SS, Pattabhi V, Gabe EJ. Structure of naproxen, $C_{14}H_{14}O_3$. Acta Crystallogr, Sect C Cryst Struct Commun. 1985;41:280–2. https://doi.org/10.1107/S0108270185003626.

58. Kistenmacher TJ, Marsh RE. Crystal and molecular structure of an antiinflammatory agent, indomethacin, 1-(p-chlorobenzoyl)-5-methoxy-2-methylindole-3-acetic acid. J Am Chem Soc. 1972;94:1340–5. https://doi.org/10.1021/ja00759a047.

59. Briard P, Rossi JC. Ketoprofene. Acta Crystallogr, Sect C: Cryst Struct Commun. 1990;46:1036–8. https://doi.org/10.1107/S0108270189004968.

60. Freer AA, Bunyan JM, Shankland N, Sheen DB. Structure of (S)-(+)-ibuprofen. Acta Crystallogr, Sect C: Cryst Struct Commun. 1993;49:1378–80. https://doi.org/10.1107/S0108270193000629.

61. Mayo SL, Olafson BD, Goddard WA. DREIDING: a generic force field for molecular simulations. J Phys Chem. 1990;94:8897–909. https://doi.org/10.1021/j100389a010.

62. Hahn M. Receptor surface models 1. Definition and construction. J Med Chem. 1995;38:2080–90. https://doi.org/10.1021/jm00012a007.

63. Molecular Operating Environment (MOE); Chemical Computing Group ULC, 1010 Sherbrooke St. West, Suite #910, Montreal, QC, Canada, H3A 2R7, 2022

64. Stewart JJP. Optimization of parameters for semiempirical methods. III Extension of PM3 to Be, Mg, Zn, Ga, Ge, As, Se, Cd, In, Sn, Sb, Te, Hg, Tl, Pb, and Bi. J Comput Chem. 1991;12:320–41. https://doi.org/10.1002/jcc.540120306.

65. Ruberte AC, Ramos-Inza S, Aydillo C, Talavera I, Encío I, Plano D, et al. Novel N, N'-disubstituted acylselenoureas as potential antioxidant and cytotoxic agents. Antioxidants. 2020;9:55. https://doi.org/10.3390/antiox9010055.

66. Plano D, Lizarraga E, Font M, Palop JA, Sanmartín C. Thermal stability and decomposition of sulphur and selenium compounds. J Therm Anal Calorim. 2009;98(2):559–66. https://doi.org/10.1007/s10973-009-0291-1.

67. Lizarraga E, Zabaleta C, Palop JA. Thermal stability and decomposition of pharmaceutical compounds. J Therm Anal Calorim. 2007;89:783–92. https://doi.org/10.1007/s10973-006-7746-4.

Authors and Affiliations

Sandra Ramos-Inza[1,2] · Eneko Almagro[3] · María Font[1,2] · Ignacio Encío[2,4] · Daniel Plano[1,2] · Carmen Sanmartín[1,2] · Rafael Sirera[3] · Elena Lizarraga[1]

✉ Elena Lizarraga
elizarraga@unav.es

[1] Department of Pharmaceutical Technology and Chemistry, University of Navarra, Irunlarrea 1, 31008 Pamplona, Spain

[2] Instituto de Investigación Sanitaria de Navarra (IdiSNA), Irunlarrea 3, 31008 Pamplona, Spain

[3] Department of Chemistry, University of Navarra, Irunlarrea 1, 31008 Pamplona, Spain

[4] Department of Health Sciences, Public University of Navarra, Avda. Barañain s/n, 31008 Pamplona, Spain